

## Studies of structural, dielectric and electrical behavior of $\text{Pb}(\text{Mn}_{1/4}\text{Co}_{1/4}\text{W}_{1/2})\text{O}_3$ ceramics

S. K. SINHA, S. N. CHOUDHARY

*University Department of Physics, T. M. Bhagpur University, Bhagalpur 812007, India*

R. N. P. CHOUDHARY

*Department of Physics and Meteorology, Indian Institute of Technology, Kharagpur 721302, India**E-mail: crnpfl@phy.iitkgp.ernet.in*

Ferroelectrics of the perovskite family having the general formula  $\text{ABO}_3$  ( $A$  = mono or divalent,  $B$  = tri, tetra, penta or hexavalent ions) have been the subject of extensive research both because of their technological importance and because of the fundamental interest in the physics of their phase transition. It is interesting to note that complex/mixed perovskite compounds formed by substituting suitable single or multi-ions at  $A$ - and/or  $B$ -sites in the above general formula have yielded many interesting physical properties useful for devices such as computer memory and display, transducers, sensors, electrostrictive actuator, microwave modulators etc. [1–4]. Further, it has been found that the desired device parameters can be obtained by suitable substitutions of single or multi-elements at the  $A$  and/or  $B$  sites of the perovskite compounds [5] satisfying the following conditions: (i) charge neutrality and (ii) suitable tolerance factor  $t$  [6], which is defined as

$$t = \frac{\bar{r}_A + r_0}{\sqrt{2}(\bar{r}_B + r_0)}$$

where  $t$  is the tolerance vector,  $\bar{r}_A$  and  $\bar{r}_B$  are the average radii of the ions at the  $A$  and  $B$  sites respectively.  $r_0 = 1.32 \text{ \AA}$  (Goldschmidt ionic radius of  $\text{O}^{2-}$ ). For ideal perovskite,  $t = 1$ . For normal or usual perovskite  $t$  is expected to be within the range  $0.80 \leq t \leq 1.05$ . From an extensive literature survey it has been found that lead-based perovskite compounds, viz  $\text{PbTiO}_3$ ,  $\text{PbZrO}_3$ , etc., have been found very important either in pure or complex forms for devices and system applications. It is also observed that not much work has been reported on modified lead tungstate and molybdate. This may be due to the higher electrical conductivity of  $\text{W}^{6+}$  and  $\text{Mo}^{6+}$  ions [7, 8]. We have controlled the conductivity effectively by substituting suitable dopants at  $B$  site [9, 10]. Here we propose to substitute isovalent cations  $\text{Mn}^{2+}$  and  $\text{Co}^{2+}$  with 25 mole percent of each individual cation at the  $W$ -site of lead tungstate to find the existence of ferroelectric properties and nature of phase transitions and conduction mechanism in them. We report here the preliminary structure and detailed electrical properties of  $\text{Pb}(\text{Mn}_{1/4}\text{Co}_{1/4}\text{W}_{1/2})\text{O}_3$  [PMCW] for better understanding of physics of materials for possible applications. The tolerance factor,  $t$  (in Pauling scale) of the compound was calculated

using the above equation and was found to be 0.89. This clearly shows that the compound should have a distorted perovskite structure.

The polycrystalline samples of PMCW were synthesized from high-purity oxides and carbonates:  $\text{PbO}$  (99.9%, M/s Aldrich Chemical Co., USA),  $\text{MnCO}_3$  (AR grade, M/s Loba Chemie Industrial Co., India);  $\text{CoCO}_3$  (99%, M/s s.d. Fine Chemical Pvt. Ltd., India) and  $\text{WO}_3$  (AR grade, M/s B.D.H. Chemical Ltd., U.K.) using a solid-state reaction technique. These ingredients taken in a suitable stoichiometry were thoroughly mixed in an agate mortar for more than 2 h. The fine mixed powder was then calcined at  $765^\circ\text{C}$  for 18 h in an alumina crucible in air atmosphere. The process of mixing and calcination was repeated until homogeneous fine powder of PMCW was obtained. Finally, the fine calcined powder of PMCW was used to make cylindrical pellets of diameter 10 mm and thickness 1–2 mm under an isostatic pressure of about  $6.5 \times 10^7 \text{ N/m}^2$ . Polyvinyl alcohol (PVA) was used as a binder to reduce the brittleness of the pellets. The binder was burnt out during the sintering of the sample. The pellets were then sintered in an alumina crucible at  $775^\circ\text{C}$  in an air atmosphere. Room temperature ( $32^\circ\text{C}$ ) X-ray diffraction pattern (XRD) of fine calcined powder were taken with a Phillips X-ray powder diffractometer (PW 1710) using  $\text{Cu K}\alpha$  radiation ( $\lambda = 1.5418 \text{ \AA}$ ) in a wide range of Bragg angles,  $2\theta$  ( $10^\circ \leq 2\theta \leq 80^\circ$ ) with a scanning rate of  $2^\circ/\text{min}$ . To study the electrical properties of the materials, both the flat surfaces of the samples were electroded with fine and air-drying silver paint and were kept at  $200^\circ\text{C}$  for 2 h to remove the moisture, if any.

The dielectric constant ( $\epsilon$ ) and loss ( $\tan \delta$ ) of PMCW were measured both as a function of frequency (1 kHz to 10 kHz) and temperature ( $32$  to  $150^\circ\text{C}$ ) using a GR 1620 AP capacitance measuring assembly and a laboratory-made 3-terminal sample holder which compensated for any stray capacitance. The dc electrical resistivity was measured both as a function of biasing electric field (9.8 kV/m to 98 kV/m) at room temperature and temperature ( $50^\circ\text{C}$  to  $350^\circ\text{C}$ ) at a constant electric field of 9.8 kV/m with the help of a Keithley-617 programmable electrometer. In the resistivity measurements the sample was first heated to above  $355^\circ\text{C}$  and then measurement was recorded in the cooling

mode. An attempt was made to study hysteresis loop of the material using Sawyer-Tower circuit [11], but no proper hysteresis loop was found because of dielectric breakdown even at low field.

The sharp and single peaks of the room temperature XRD pattern of PMCW, which were different in position and intensity from those of ingredient carbonate and oxides, suggested the formation of single-phase compound. All the reflections (strong, medium and weak) were indexed and the lattice parameters were determined in different crystal systems and cell configurations using a computer package Program "Powd-Mult". A very good agreement between  $d_{\text{obs}}$  and  $d_{\text{cal}}$  was observed in the orthorhombic crystal system. Finally, the lattice parameters were refined using the least-squares method. The refined lattice parameters are:  $a = 10.4387(20)$  Å,  $b = 12.6326(20)$  Å and  $c = 13.7269(20)$  Å. The  $d_{\text{obs}}$  and  $d_{\text{cal}}$  of PMZW have been compared in Table I. With limited number of reflections of XRD pattern, it was not possible to determine the space group of the material. Using the XRD pattern and Scherrer's equation [12] [ $P_{\text{hkl}} = k\lambda/\beta_{1/2}\text{Cos } \theta_{\text{hkl}}$  where  $k = 0.89$  and  $\beta_{1/2} = \text{half peak width}$ ], coherently scattered particle size of the compound was calculated and was found to be 189 Å. The smaller particle size is of a great importance, as it offers a higher rate of densification due to both an increase in driving force for sintering and to the smaller distances of mass transport needed to fill the pores, thus permitting lowering of sintering temperature and the achievement of fine grain ceramics.

Fig. 1 shows the variations of the dielectric constant ( $\epsilon$ ) and dielectric loss ( $\tan \delta$ ) as a function of frequency at room temperature. The nature of the variation of these parameters shows the expected behavior of a dielectric. The dielectric constant decreases with increasing fre-

TABLE I Comparison of observed and calculated  $d$ -values (in Å) of some reflections of  $\text{Pb}(\text{Mn}_{1/4}\text{Co}_{1/4}\text{W}_{1/2})\text{O}_3$  compound at room temperature

$h$	$k$	$l$	$d_{\text{obs}}$	$d_{\text{cal}}$	$I/I_0$
0	1	1	9.2779	9.2954	6
0	0	3	4.5800	4.5756	7
3	0	0	3.4802	3.4796	68
3	0	1	3.3671	3.3729	16
1	0	4	3.2641	3.2601	100
0	4	1	3.0833	3.0777	38
1	4	0	3.0235	3.0228	27
1	2	4	2.9104	2.8970	27
0	0	5	2.7409	2.7454	28
2	4	1	2.6456	2.6511	11
2	0	6	2.0953	2.0954	17
2	6	1	1.9330	1.9331	25
1	4	6	1.8244	1.8242	10
0	3	7	1.7771	1.7777	15
4	4	4	1.7364	1.7355	12
6	1	1	1.7123	1.7101	13
2	3	7	1.6825	1.6828	16
4	2	6	1.6592	1.6599	22
6	0	3	1.6256	1.6262	17
5	4	4	1.5526	1.5530	12
2	4	8	1.4484	1.4485	9
6	5	0	1.4329	1.4329	36
6	2	6	1.3525	1.3527	8

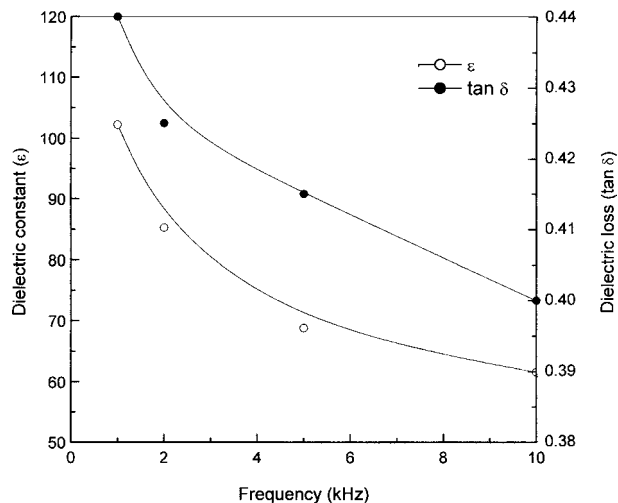


Figure 1 Variation of dielectric constant ( $\epsilon$ ) and dielectric loss ( $\tan \delta$ ) of PMCW as a function of frequency at room temperature.

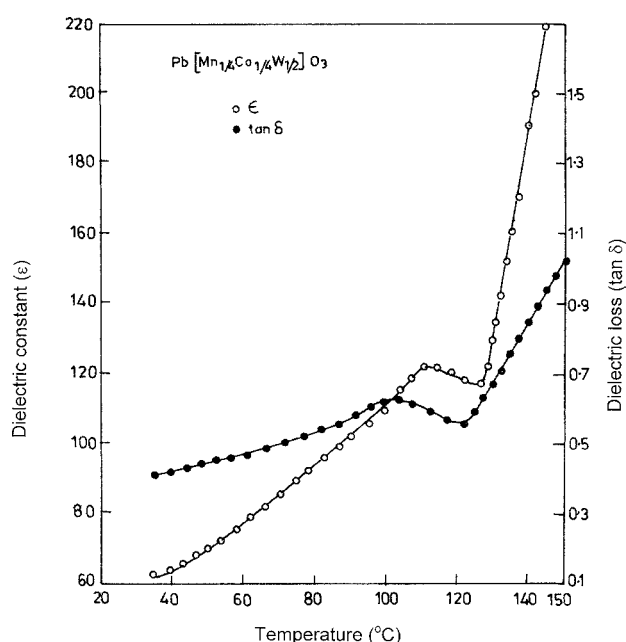


Figure 2 Variation of dielectric constant ( $\epsilon$ ) and dielectric loss ( $\tan \delta$ ) of PMCW as a function of temperature at 10 kHz.

quency. This suggests the presence of different types of polarizations (i.e., electronic, atomic, dipolar, orientational etc.) at low frequencies. As frequency is increased, some of the polarizations are ineffective, and hence we have a lower value of  $\epsilon$ .

Fig. 2 shows the variation of  $\epsilon$  and  $\tan \delta$  as a function of temperature (32–50 °C) at 10 kHz. From this plot it is clear that the compound has a weak dielectric anomaly at 108 °C (usually referred as  $T_c$ ). Above 128 °C,  $\epsilon$  increases sharply with further rise in temperature. This is due to the presence of space charge polarization in the bulk material. The dielectric loss varies in a similar way. A small temperature difference between the peaks of dielectric constant and loss tangent is consequently an outcome of Kramers-Kronig relation accounting for the broadening of phase transition in the material [13]. Further,  $\text{Mn}^{2+}$ ,  $\text{Co}^{2+}$  and  $\text{W}^{6+}$  ions occupy octahedral positions. This suggests that in PMCW, the fluctuations in the statistical distribution of  $\text{Mn}^{2+}$ ,  $\text{Co}^{2+}$  and  $\text{W}^{6+}$

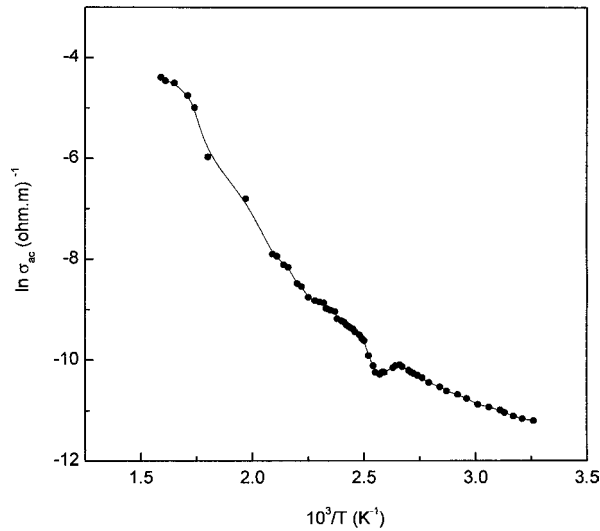


Figure 3 Variation of ac conductivity ( $\ln \sigma_{ac}$ ) of PMCW as a function of inverse of absolute temperature ( $10^3/T$ ) at 10 kHz.

are too small to be conspicuous for providing a fairly broadened phase transition.

The ac electrical conductivity ( $\sigma_{ac}$ ) and activation energy ( $E_a$ ) of PMCM in the paraelectric phase were calculated from the measured dielectric data and using the formulate [14]  $\sigma_{ac} = \varepsilon \varepsilon_0 \omega \tan \delta$ —(1) and  $\sigma_{ac} = \sigma_0 \exp. (-E_a/k_B T)$ —(2) where  $\varepsilon_0$  is the vacuum dielectric constant,  $\omega$  the angular frequency and  $k_B$  the Boltzmann constant. The plot of Equation 2 as in  $\sigma_{ac}$  versus  $10^3/T$  is shown in Fig. 3. The small hump observed at  $108^\circ\text{C}$  is in consistent with the transition temperature observed in our dielectric studies. This confirmed a phase transition in the compound. This type of observation has been found in many other oxide ferroelectrics [10, 15, 16]. In spite of this anomaly in dielectric constant and ac conductivity, proper hysteresis loop was not observed. Attempts are being made again to modify the Sawyer-Tower circuit for the purpose. The activation energy was found to be 0.56 eV. The low activation energy can be explained as follows: Typical ionic solids possess a limited number of mobile ions, which are hindered in their motion by being trapped in relatively stable potential walls. Due to a rise in temperature the donor cations take a major part in conduction. The donors create a level (usually called a donor level) in the vicinity of the conduction band. Therefore, to activate donors a small amount of energy is required. In addition to this, a slight change in stoichiometry (i.e., the metal : oxygen ratio) in multi metal complex oxides causes the creation of a large number of donors or acceptors, which create donor-or acceptor-like states in the vicinity of conduction or valence bands. These donors or acceptor can be activated even with little energy [17].

The variation of dc resistivity ( $\rho_{dc}$ ) with the biasing field at room temperature is shown in Fig. 4. The dc resistivity of the material decreases with increase in biasing field. With direct applied voltage, the diffusion of mobile impurity ions builds up a much larger charge at the surface until the reverse field so developed from the surface charge eventually arrests the current. As such, with increase in dc field the surface charge build

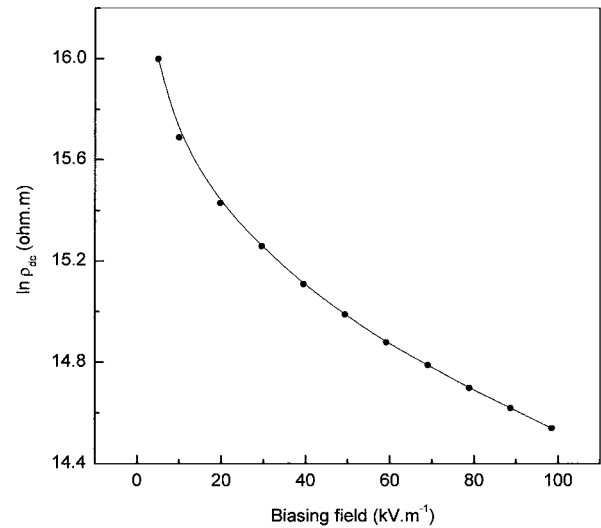


Figure 4 Variation of dc resistivity ( $\ln \rho_{dc}$ ) of PMCW as a function of biasing field at room temperature.

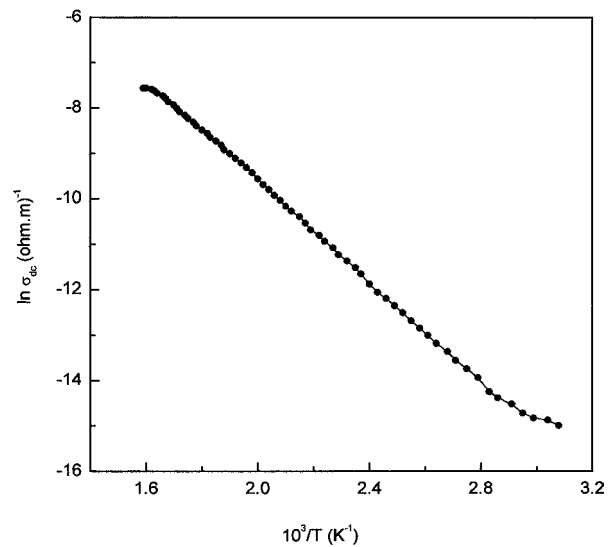


Figure 5 Variation of dc conductivity ( $\ln \sigma_{dc}$ ) of PMCW as a function of temperature at a constant electric field 9.8 kV/m.

up by the mobile ions is expected to increase which explains the nature of  $\rho_{dc}$  versus biasing field curve.

Fig. 5 shows the variation of dc conductivity ( $\sigma_{dc}$ ) of PMCW with temperature at a constant biasing field of 9.8 kV/m. The increase in conductivity at high temperature may, however, be possibly due to the supply of more and more thermal energy to the material as the temperature increases. This results in the creation of more and more free electrons that could be set free from  $\text{O}^{2-}$  ions. When an electron is introduced in the sample it might be associated with cations, which results in creating an unstable valence state [18]. This type of resistive behavior is found in many ferroelectric materials studied by us [19–21]. The activation energy ( $E_a$ ) of PMCW compound calculated from the slope of the  $\ln \sigma_{dc}$  versus  $10^3/T$  was found to be 0.51 eV in the higher temperature region. From low value of activation energy, it is again confirmed that oxygen may be the main carrier in the electrical conduction.

Finally, it is concluded that PMCW has orthorhombic structure at room temperature and undergoes weak

dielectric anomaly at 108 °C. At higher temperature PMCW shows semiconducting behavior and can be effectively used for highly sensitive thermal detectors, sensors, thermistors etc.

## References

1. T. NEGAS, G. YEAGER, S. BELL and N. COATS, *Amer. Ceram Soc. Bull.* **72** (1993) 80.
2. H. TAMURA, T. KONOLLE, Y. SAKABLE and K. WAKINO, *J. Amer. Ceram. Soc.* **67** (1989) C59.
3. K. WAKINO, K. MINAI and H. TAMURA, *ibid.* **67** (1984) 278.
4. D. VIEHLAND, N. KIM, Z. XU and D. A. PAYNE, *ibid.* **78** (1995) 2481.
5. G. A. SMOLENSKII, A. I. AGRANOVSKAYA and V. A. ISUPOV, *Sov. Phys. Solid State* **1** (1959) 907.
6. B. JAFEE, JR., W. R. COOK and H. JAFEE, "Piezoelectric Ceramics" (Academic Press, New York, 1971).
7. F. JONA and G. SHIRANE, "Ferroelectric Crystal" (Pergamon, Germany, 1962).
8. S. N. BAI and T. Y. TSENG, *J. Appl. Phys.* **74** (1993) 695.
9. S. K. SINHA, R. N. P. CHOUDHARY, S. N. CHOUDHARY and T. P. SINHA, *Mater. Lett.* **51** (2001) 336.
10. S. K. SINHA, S. N. CHOUDHARY and R. N. P. CHOUDHARY, *J. Electroceram.* **7** (2001) 121.
11. J. K. SINHA, *J. Sci. Instrum.* **42** (1965) 696.
12. H. B. KLUNG and L. B. ALEXANDER, "X-ray Diffraction Procedures" (Wiles, New York, 1974).
13. M. E. LINES and A. M. GLASS, "Principles and Applications of Ferroelectrics and Related Materials" (Clarendon Press, Oxford, 1977) p. 138.
14. J. C. ANDERSON, "Dielectrics" (Chapman and Hall, London, 1964).
15. S. K. SINHA, R. N. P. CHOUDHARY, S. N. CHOUDHARY and T. P. SINHA, *J. Phys. Chem. Solids.* **63** (2002).
16. S. K. SINHA, S. N. CHOUDHARY and R. N. P. CHOUDHARY, *Mater. Chem. Phys.* **70** (2001) 296.
17. R. C. BUCHANAN, "Ceramic Materials for Electronics" (Marcel Dekker, New York, 1986).
18. N. B. HUNNY, "Semiconductors" (Reinhold Publishing Corp., New York, 1959).
19. S. K. SINHA, S. N. CHOUDHARY and R. N. P. CHOUDHARY, *J. Mater. Sci. Lett.* **22** (2003) 21.
20. *Idem.*, *Ind. J. P. Appl. Phys.* **40** (2002) 277.

Received 14 July  
and accepted 29 July 2003